Spontaneous Spin Textures in Multiorbital Mott Systems

J. Kuneš[1,*] and D. Geffroy[2]
[1]Institute of Physics, The Czech Academy of Sciences, Na Slovance 2, 182 21 Praha 8, Czech Republic
[2]Department of Condensed Matter Physics, Faculty of Science, Masaryk University, Kotlářská 2, 611 37 Brno, Czech Republic
(Received 29 February 2016; revised manuscript received 4 May 2016; published 22 June 2016)

Spin textures in **k**-space arising from spin-orbit coupling in noncentrosymmetric crystals find numerous applications in spintronics. We present a mechanism that leads to the appearance of **k**-space spin texture due to spontaneous symmetry breaking driven by electronic correlations. Using dynamical mean-field theory we show that doping a spin-triplet excitonic insulator provides a means of creating new thermodynamic phases with unique properties. The numerical results are interpreted using analytic calculations within a generalized double-exchange framework.

DOI: 10.1103/PhysRevLett.116.256403

Manipulation of spin polarization by controlling charge currents and vice versa has attracted considerable attention due to applications in spintronic devices. A major role is played by spin-orbit (SO) coupling in noncentrosymmetric systems. As originally realized by Dresselhaus [1] and Rashba [2], SO coupling in a noncentrosymmetric crystal lifts the degeneracy of the Bloch states at a given **k**-point and locks their momenta and spin polarizations together giving rise to a spin texture in reciprocal space. This leads to a number of phenomena [3] such as spin torques in ferro- [4,5] and antiferromagnets [6,7], topological states of matter, or spin textures in the reciprocal space that are the basis of the spin galvanic effect [8]. Electronic correlations alone can provide coupling between spin polarization and charge currents, e.g., via effective magnetic fields acting on electrons moving through a noncoplanar spin background [9,10]. Wu and Zhang [11] proposed that SO coupling can be generated dynamically in analogy to the breaking of relative spin-orbit symmetry in ^{3}He [12]. Subsequently, an effective field theory of spin-triplet Fermi surface instabilities with high orbital partial wave was developed in Ref. [13].

Here, we present a spontaneous formation of a **k**-space spin texture, similar to the effect of Rashba-Dresselhaus SO coupling, in centrosymmetric bulk systems with no intrinsic SO coupling. The spin texture is a manifestation of excitonic magnetism that has been proposed to take place in some strongly correlated materials [14,15]. The basic ingredient is a crystal built of atoms with quasidegenerate singlet or triplet ground states. Under suitable conditions a spin-triplet exciton condensate [16,17] is formed, which may adopt a variety of thermodynamic phases with diverse properties [18]. Several experimental realizations of excitonic magnetism have already been discussed in the literature [19–23].

Model.— We use the dynamical mean-field theory (DMFT) to study the minimal model of an excitonic magnet—the two-orbital Hubbard Hamiltonian at half-filling

$$
\begin{aligned}
H &= \sum_{\langle ij\rangle} H_t^{(ij)} + \frac{\Delta}{2}\sum_{i\sigma}(n^a_{i\sigma} - n^b_{i\sigma}) + \sum_i H^{(i)}_{\rm int},\\
H^{(i)}_{\rm int} &= U(n^a_{i\uparrow}n^a_{i\downarrow} + n^b_{i\uparrow}n^b_{i\downarrow}) + U'\sum_{\sigma\sigma'} n^a_{i\sigma}n^b_{i\sigma'}\\
&\quad - J\sum_{\sigma}(n^a_{i\sigma}n^b_{i\sigma} + \gamma a^\dagger_{i\sigma}a_{i-\sigma}b^\dagger_{i-\sigma}b_{i\sigma}).
\end{aligned}
\tag{1}
$$

The local part of the Hamiltonian contains the crystal-field splitting Δ between the orbitals labeled a and b and the Coulomb interaction with ferromagnetic Hund's exchange J. The kinetic part H_t describes the nearest-neighbor hopping on the square lattice between the same orbital flavors t_a, t_b as well as cross-hopping between the different orbital flavors V_1, V_2; see Fig. 1. The parameters Δ and J are balanced such that the energy difference between the atomic low-spin (LS) and high-spin (HS) states is smaller or comparable to the kinetic energy gain due to the electron delocalization. The numerical simulations using continuous-time quantum Monte Carlo impurity solver [24,25] were performed with the density-density approximation for the interaction ($\gamma = 0$), which effectively introduces a magnetic easy axis in the present model. Analytic mean-field calculations as well as preliminary DMFT

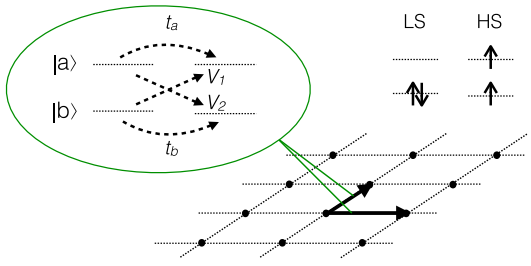

FIG. 1. The hopping processes with corresponding amplitudes on the square lattice. The parameters used in the calculations: $t_a = 0.4118$, $t_b = -0.1882$, $V_1 = \pm V_2 = 0.05$, $\Delta = 3.4$, $U = 4$, $U' = 2$, and $J = 1$ in units of eV.

computations performed with the SU(2) symmetric model [18] show only quantitative differences (e.g., reduction of the transition temperature). The spectral functions were obtained using the maximum entropy method [26]. Technical details can be found in the Supplemental Material [27].

Studies [15,19,28–31] performed without cross-hopping $V_{1,2} = 0$ revealed formation of the exciton condensate below a critical temperature, which decreases with doping away from integer filling. In the strong-coupling limit the ground state wave function of a uniform condensate can be approximated by a product of local functions $\Pi_i |C_i\rangle$ with each $|C\rangle = s b_\uparrow^\dagger b_\downarrow^\dagger + \xi_1 a_\uparrow^\dagger b_\uparrow^\dagger + (\xi_0/\sqrt{2})(a_\uparrow^\dagger b_\downarrow^\dagger + a_\downarrow^\dagger b_\uparrow^\dagger) + \xi_{-1} a_\downarrow^\dagger b_\downarrow^\dagger |\mathrm{v}\rangle$ [32], describing a local hybrid between the LS and HS states with amplitudes s, ξ_1, ξ_0, and ξ_{-1}, which provides a useful analytic reference for interpretation of the numerical results. In the DMFT calculations we characterize the thermodynamic phases by the order parameter $\boldsymbol{\phi}^{(i)} = \sum_{\alpha\beta} \boldsymbol{\sigma}_{\alpha\beta} \langle a_{i\alpha}^\dagger b_{i\beta} \rangle$, with Pauli matrices $\boldsymbol{\sigma}$. In addition, we evaluate the spin moment per atom $\mathbf{M}$ as well as the spin density in the direct space $\mathbf{m}(\mathbf{r})$ [33] and in the reciprocal space $\mathbf{m}_\mathbf{k} = \sum_{\alpha\beta} \boldsymbol{\sigma}_{\alpha\beta} \langle a_{\mathbf{k}\alpha}^\dagger a_{\mathbf{k}\beta} + b_{\mathbf{k}\alpha}^\dagger b_{\mathbf{k}\beta} \rangle$.

In Fig. 2 we show the phase diagrams of Eq. (1) as functions of temperature T and hole doping n_h away from $n = 2$. We choose the hopping parameters so that $t_a t_b < 0$ which leads to a uniform $\boldsymbol{\phi}$-order. Note that on a bipartite lattice the $t_a t_b > 0$ case with a staggered $\boldsymbol{\phi}$-order can be mapped on the $t_a t_b < 0$ by the gauge transformation $a_i \to (-1)^i a_i$ [18]. We consider two cross-hopping patterns at this point: $V_1 = V_2$ (even) and $V_1 = -V_2$ (odd). The two corresponding phase diagrams share the general features inherited from the "parent" system with no cross-hopping studied in Ref. [28]. These include the polar state with no ordered moments at low doping levels and a doping-induced transition to a different excitonic phase. The thermodynamic phase can be distinguished by several criteria. The ferromagnetic condensate (FMEC) has the oder parameter of the form $\boldsymbol{\phi} = \mathbf{x} + i\mathbf{x}'$ (with noncollinear real vectors $\mathbf{x}$ and $\mathbf{x}'$), which generates a finite uniform polarization $M_\perp$ perpendicular to $\boldsymbol{\phi}$. The order parameter in polar condensates can be written as $\boldsymbol{\phi} = e^{i\varphi}\mathbf{x}$ (real vector $\mathbf{x}$ times an arbitrary scalar phase φ). The polar condensates can be further distinguished by their time-reversal (TR) symmetry into the spin-density-wave (SDW; real $\boldsymbol{\phi}$; breaks TR) and spin-current-density-wave (SCDW; imaginary $\boldsymbol{\phi}$; preserves TR) types, introduced by Halperin and Rice [16]. The SDW order gives rise to a finite intra-atomic spin polarization $\mathbf{m}(\mathbf{r})$—higher magnetic multipole—while the SCDW order gives rise to intra-atomic spin current with $\mathbf{m}(\mathbf{r}) = 0$ [34]. The preference of the undoped system for SDW or SCDW ordering on a given bond is controlled by the sign of $t_a t_b V_1 V_2$ and follows the rules given in Ref. [15]. Finally, we distinguish the polar phases into the primed and unprimed ones. The spin(current) polarization in the unprimed phases is purely local, reflected by $\mathbf{m}_\mathbf{k} = 0$. The primed phase are characterized by appearance of $\mathbf{k}$-space spin textures, $\mathbf{m}_\mathbf{k} \neq 0$, which in case of SCDW′ phase represents global spin currents. The characteristics for the different phases are summarized in Table I.

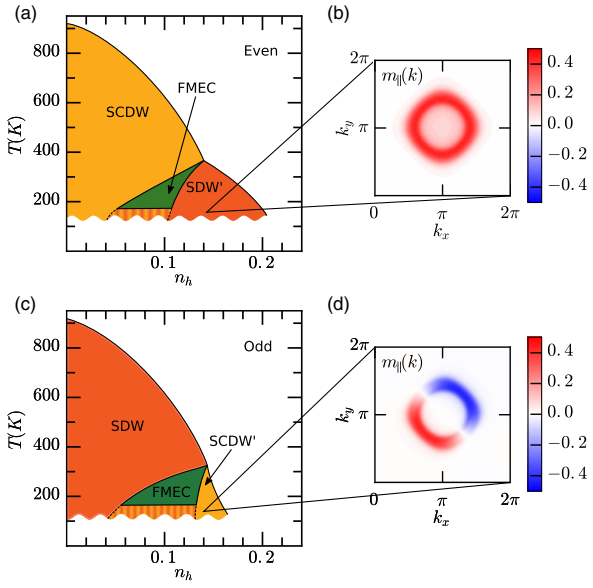

FIG. 2. (a) and (c) Phase diagrams in the doping-temperature plane for even and odd cross hopping, respectively. Full lines mark continuous transitions, dotted lines mark the boundaries of phase coexistence regions. (b) and (d) The spin textures at the indicated points of the phase diagrams in the units of $\mu_B(a_0/2\pi)^2$ obtained for $n_h = 0.14$ at $T = 193$ K.

Double-exchange mechanism.— Observation of the spontaneous spin textures in the primed phases is our central result. It can be understood by invoking the generalized double-exchange mechanism, recently used by Chaloupka and Khaliullin to study ruthenates [35]. Analogous to the well-known Zener double exchange [36] in manganites, the exciton condensate acts as a filter for propagation of doped carriers. The stable phase is determined by the competition between the kinetic energy of doped carriers and the energy difference between possible condensates. In the strong coupling limit, propagation

TABLE I. The characteristics of different condensate phases: $M_\perp$ and $M_\parallel$ is magnetic moment per atom perpendicular and parallel to the order parameter $\boldsymbol{\phi}$, respectively; $\mathbf{m}(\mathbf{r})$ and $\mathbf{m}_\mathbf{k}$ are the spin densities in direct and reciprocal space, respectively. By ✓/0 we indicate that both cases may be realized (see the text).

Condensate state	$M_\perp$	$M_\parallel$	$\mathbf{m}(\mathbf{r})$	$\mathbf{m}_\mathbf{k}$	Re$\boldsymbol{\phi}$	Im$\boldsymbol{\phi}$
FMEC	✓	✓/0	✓	✓	✓	✓
SDW	0	0	✓	0	✓	0
SCDW	0	0	0	0	0	✓
SDW'	0	✓/0	✓	✓	✓	0
SCDW'	0	0	0	✓	0	✓

of a single electron through the condensate with order parameter $\boldsymbol{\phi}^{(i)}$ is described by an effective Hamiltonian (see the Supplemental Material [27] for the derivation)

$$H_{\text{eff}} = \sum_{\langle ij \rangle} \left(t_s \delta_{\alpha\beta} + \frac{1}{2} \mathbf{B}^{(ij)} \cdot \boldsymbol{\sigma}_{\alpha\beta} \right) \tilde{b}^{\dagger}_{i\alpha} \tilde{b}_{j\beta} + \text{H.c.}$$

with

$$\mathbf{B}^{(ij)} = \frac{i t_a}{2 s^2} (\boldsymbol{\phi}^{(j)} \wedge \boldsymbol{\phi}^{(i)*}) + V_1^{(ji)} \boldsymbol{\phi}^{(j)} + V_2^{(ji)} \boldsymbol{\phi}^{(i)*} \qquad (2)$$

and $t_s = -t_b s^2 - t_a (1 - s^2)$. Here, $\boldsymbol{\sigma}$ are the Pauli matrices and s^2 is the LS fraction in the condensate. In general, the $\mathbf{B}$ fields depend on the site indices as indicated in the brackets—in the studied "odd" and "even" models the site indices are obsolete.

The ϕ-quadratic term in Eq. (2) describes the standard double-exchange interaction of the doped particle with the uniform background with spin polarization $\mathbf{M}_{\perp} = -i(\boldsymbol{\phi}^* \wedge \boldsymbol{\phi})/s^2$ [37]. At low doping the antiferromagnetic interactions between the HS states dominate, rendering the system a polar condensate with spin-independent hopping in Eq. (2). For some critical doping, however, the gain in the kinetic energy of doped carriers in FMEC outweighs the cost in the HS-HS exchange energy and the system adopts the FMEC state.

The ϕ-linear term in Eq. (2), which dominates at least close to the normal-phase boundary, appears only with finite cross-hopping in the condensate phase. The strong coupling calculations [15] (see the Supplemental Material [27]) show that the V_1 and V_2 contributions in Eq. (2) cancel out, $V_1 \boldsymbol{\phi} + V_2 \boldsymbol{\phi}^* = 0$, for $\boldsymbol{\phi}$ that minimizes the bond energy. On a bipartite lattice, where all bonds can be satisfied simultaneously, the ϕ-linear term vanishes globally, allowing the SDW and SCDW phases at finite doping.

When kinetic energy gain of the doped particles overcomes the interactions selecting the condensate type in the undoped system, the ϕ-linear term in Eq. (2) becomes finite. It has a form of an exchange field acting on bonds or equivalently acting locally in the reciprocal space, which for the two hopping patterns considered so far reads

$$\mathbf{B}_{\mathbf{k}} = 4 V_1 \boldsymbol{\phi} \begin{cases} \cos k_x + \cos k_y & \text{SDW}' \\ i(\sin k_x + \sin k_y) & \text{SCDW}' \end{cases} \qquad (3)$$

More generally, the $\mathbf{B}_{\mathbf{k}}$ reflects the symmetry of the cross-hopping pattern. The s-wave symmetry of our even cross hopping therefore leads to an s-wave texture, Fig. 2, with a finite $M_{\parallel}$. Apart from strong radial localization, the $\mathbf{m}_{\mathbf{k}}$ is not qualitatively different from an approximately constant $\mathbf{m}_{\mathbf{k}}$ of normal local moment ferromagnet. However, a d-wave cross hopping, with V's along the x and y directions having opposite signs, produces a d-wave texture, shown in Fig. 3, and $M_{\parallel} = 0$. We point out that without doping the s- and d-wave systems are identical, in the strong-coupling limit, since the cross-hopping enters as a product $V_1 V_2$ on each bond [15].

The SCDW′ phase is characterized by purely imaginary $\boldsymbol{\phi}$, which gives rise to the $\mathbf{k}$-odd exchange field in Eq. (3). The odd cross-hopping pattern can be thought of as having $p_x + p_y$ symmetry, which is imprinted in the spin texture, shown in Fig. 2(b). There is not only no net polarization $\mathbf{M} = 0$, but the polarization is zero in every point $\mathbf{m}(\mathbf{r}) = 0$ [27] reflecting the TR invariance of the SCDW′ state. In Fig. 4 we analyze spin texture in the SCDW′ state in detail. The frequency-resolved contributions to $\mathbf{m}_{\mathbf{k}}$ in Figs. 4(c) and 4(d) reveal that the spin polarization comes from a narrow energy range around the Fermi level. Spectral functions exhibit rather sharp quasiparticle bands around the Fermi level resembling a band structure of noninteracting system. The spin density, on the other hand, is quite different from that of a noninteracting system. It cannot be associated with particular quasiparticle bands but rather lives on their tails in sharply defined regions of the Brillouin zone.

The shape of the spin texture in the SCDW′ state is determined by the model parameters. Its collinear polarization, similar to equal combination of Rashba and Dresselhaus SO coupling [3], is picked randomly at the transition. The Weiss field in the SCDW and SCDW′ phases, which generates local intra-atomic spin currents, can be viewed as spontaneously generated SO coupling. The corresponding "SO" splitting is approximately $(U - 2J)|\phi|$, thus can be as large as lower units of eV. Only in the SCDW′ phase the spontaneous SO coupling is taken to the inter-atomic scale. The equivalent of Rashba-Dresselhaus SO coupling is found in Eq. (3) with the largest amplitude, in the (1,1) direction, of $4V_1|\phi|a_0$. With $|\phi| \sim 0.2 - 0.4$ (maximum theoretical value is $1/\sqrt{2}$), the present cross hopping of 50 meV, and the lattice constant a_0 of a few Å the effective Rashba-Dresselhaus SO constant is of the order 1×10^{-11} eV m.

Realization.— To support the SDW′ or SCDW′ states a material (i) must exhibit spin-triplet polar exciton

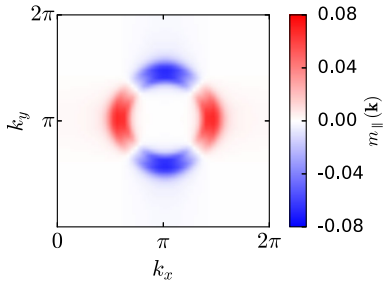

FIG. 3. The d-wave spin texture in the SDW′ phase of a model with even cross hopping of opposite signs along the x and y axes. The results shown here were obtained for $n_h = 0.16$ at $T = 193$ K.

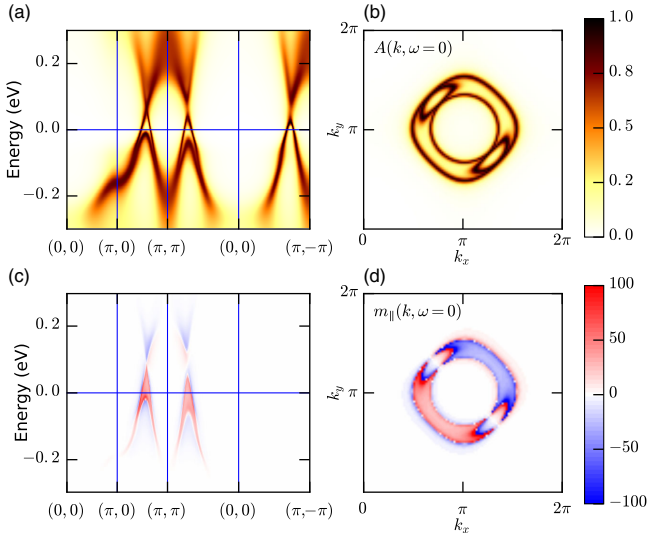

FIG. 4. One-particle spectral density in the SCDW′ phase for the same parameters as Fig. 2(d): (a) Total spectral density $A(\mathbf{k},\omega)$ along high-symmetry lines in the Brillouin zone, (b) the Fermi surface $A(\mathbf{k},\omega=0)$, (c) in-plane magnetization spectral density $m_\parallel(\mathbf{k},\omega)$ along the same lines as in panel (a), (d) in-plane magnetization density at the Fermi level $m_\parallel(\mathbf{k},\omega=0)$ in the units of $\mu_B \mathrm{eV}^{-1}(a_0/2\pi)^2$.

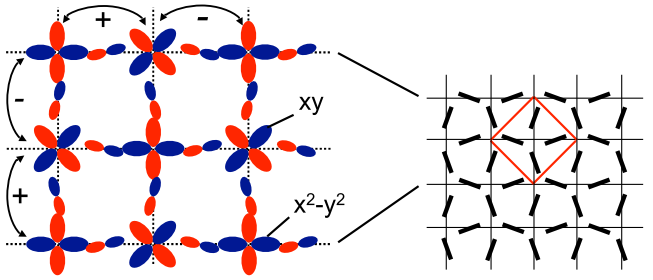

FIG. 5. A cartoon view of the orbital pattern (left) that gives rise to $t_a, t_b > 0$ and $V_1 = V_2$ on each bond with alternating signs between bonds (only half of the orbitals are shown for the sake of clarity). Zoomed out view of the texture on the ligand sublattice (right). The red square marks the crystallographic unit cell. The model can be transformed to the odd cross-hopping case with a single-atom unit cell by sublattice transformation $a_i \to (-1)^i a_i$.

condensation, (ii) the local SDW or SCDW must give rise to spin-dependent hopping in Eq. (3), and (iii) the spin-dependent hopping must generate a global pattern spin polarization or spin currents.

Transition metal perovskites are the most discussed candidates for excitonic magnetism [14,19,21]. The singlet-triplet quasidegeneracy favorable for (i) is typically realized in d^6 configuration in octahedral geometry (Fe^{2+}, Co^{3+}, Ni^{4+}), d^8 configuration in square planar geometry (Ni^{2+}), or d^4 configuration in octahedral geometry with strong spin-orbit coupling (Ru^{4+}, Os^{4+}, Rh^{5+}, Ir^{5+}). Therefore, we focus on models built of d orbitals.

It is quite straightforward to construct the even (or d-wave) model and thus the SDW′ state from orbitals of the same parity. We focus on the more difficult odd model and the SCDW′ state. Here we propose two options. First, we use the fact that only the in-plane parity is relevant. We can start with lattice of $3z^2 - r^2$ (or $x^2 - y^2$) and $z(x + y)$ orbitals. Breaking of the $z \leftrightarrow -z$ symmetry, e.g., by a substrate leads to the desired odd cross-hopping pattern.

The second option is a model built of $x^2 - y^2$ and xy orbitals with more than one atom in the unit cell. In this case, the conditions (ii) and (iii) become distinct. For example, one can obtain $V_1 V_2 < 0$ on each bond by tilting the orbitals (oxygen octahedral in real perovskite). However, the corresponding pattern of $\mathbf{B}^{(ij)}$ has alternating signs and does not give rise to a finite $\mathbf{m}_\mathbf{k}$. In order to create the desired cross-hopping pattern the inversion centered at the atomic site has to be removed. In Fig. 5 we show an example of such hopping pattern in an Emery-like model.

The diagonal hopping amplitudes t_a and t_b are both negative. The cross hopping (V_1, V_2), via tilted oxygen orbitals (induced for example by a substrate with appropriate texture), follows the $(++), (--), (++), \ldots$ pattern along both the x and y directions. These suggestions are obviously not the only ways to realize hopping patterns favoring the SCDW′ phase.

The currently most advanced experimental realization of the triplet-excitonic condensation is perhaps the Ca_2RuO_4 [21] described by the model of Khaliullin [14], which is equivalent to the strong coupling limit of the present model for a special choice of parameters. While the double-exchange mechanism is active also in ruthenates [35], static spin textures were not reported. Since the equivalents of cross- and diagonal hopping in ruthenates originate from the same $t_{2g} \to t_{2g}$ process, their ratio is fixed and close to 1. This is quite different from the present parameters with small cross hopping.

Finally, we point out that $\mathbf{k}$-space spin textures are accessible in cold atoms experiments, where the two-orbital model may be sufficiently simple to realize.

In conclusion, we have presented the doping of exciton condensates in systems of strongly correlated electrons as a way to generate unique states of matter. The generalized double-exchange mechanism in these systems can give rise to exchange fields that act on the itinerant electrons in the reciprocal space. The actual existence of such fields depends on the particular thermodynamic phase and crystal symmetry. In the studied model we found a broken-symmetry state with a $\mathbf{k}$-space spin texture with a symmetry of an equal combination of Rashba and Dresselhaus SO couplings.

We thank G. Khaliullin, A. Hariki, L. H. Tjeng, and V. Pokorný for discussions, and A. Sotnikov and A. Kauch for critical reading of the manuscript. J. K. received funding from the European Research Council under the European Union's Horizon 2020 research and innovation

programme (Grant Agreement No. 646807) and Deutsche Forschungsgemeinschaft under Forschergruppe FOR1346. D. G. was supported by projects MUNI/A/1496/2014 and MUNI/A/1388/2015 of the Masaryk University.

*kunes@fzu.cz

[1] G. Dresselhaus, Phys. Rev. **100**, 580 (1955).
[2] E. Rashba, Sov. Phys. Solid State **2**, 1109 (1960).
[3] A. Manchon, H. C. Koo, J. Nitta, S. M. Frolov, and R. A. Duine, Nat. Mater. **14**, 871 (2015).
[4] A. Manchon and S. Zhang, Phys. Rev. B **78**, 212405 (2008).
[5] H. Li, H. Gao, L. P. Zârbo, K. Výborný, X. Wang, I. Garate, F. Doğan, A. Čejchan, J. Sinova, T. Jungwirth *et al.*, Phys. Rev. B **91**, 134402 (2015).
[6] J. Železný, H. Gao, K. Výborný, J. Zemen, J. Mašek, A. Manchon, J. Wunderlich, J. Sinova, and T. Jungwirth, Phys. Rev. Lett. **113**, 157201 (2014).
[7] P. Wadley, B. Howells, J. Železný, C. Andrews, V. Hills, R. P. Campion, V. Novák, K. Olejník, F. Maccherozzi, S. S. Dhesi *et al.*, Science **351**, 587 (2016).
[8] J. Wunderlich, A. C. Irvine, J. Sinova, B. G. Park, L. P. Zârbo, X. L. Xu, B. Kaestner, V. Novák, and T. Jungwirth, Nat. Phys. **5**, 675 (2009).
[9] N. Nagaosa, X. Z. Yu, and Y. Tokura, Phil. Trans. R. Soc. A **370**, 5806 (2012).
[10] F. Jonietz, S. Mühlbauer, C. Pfleiderer, A. Neubauer, W. Münzer, A. Bauer, T. Adams, R. Georgii, P. Böni, R. A. Duine *et al.*, Science **330**, 1648 (2010).
[11] C. Wu and S.-C. Zhang, Phys. Rev. Lett. **93**, 036403 (2004).
[12] D. Vollhardt and P. Wölfle, *The Superfluid Phases of Helium 3* (Dover, New York, 2013), reprint ed.
[13] C. Wu, K. Sun, E. Fradkin, and S.-C. Zhang, Phys. Rev. B **75**, 115103 (2007).
[14] G. Khaliullin, Phys. Rev. Lett. **111**, 197201 (2013).
[15] J. Kuneš and P. Augustinský, Phys. Rev. B **89**, 115134 (2014).
[16] B. I. Halperin and T. M. Rice, *Solid State Physics* (Academic, New York, 1968), Vol. 21, p. 115.
[17] L. Balents, Phys. Rev. B **62**, 2346 (2000).
[18] J. Kuneš, J. Phys. Condens. Matter **27**, 333201 (2015).
[19] J. Kuneš and P. Augustinský, Phys. Rev. B **90**, 235112 (2014).
[20] G. Cao, T. F. Qi, L. Li, J. Terzic, S. J. Yuan, L. E. DeLong, G. Murthy, and R. K. Kaul, Phys. Rev. Lett. **112**, 056402 (2014).
[21] A. Jain, M. Krautloher, J. Porras, G. H. Ryu, D. P. Chen, D. L. Abernathy, J. T. Park, A. Ivanov, J. Chaloupka, G. Khaliullin *et al.*, arXiv:1510.07011.
[22] T. Dey, A. Maljuk, D. V. Efremov, O. Kataeva, S. Gass, C. G. F. Blum, F. Steckel, D. Gruner, T. Ritschel, A. U. B. Wolter *et al.*, Phys. Rev. B **93**, 014434 (2016).
[23] K. Pajskr, P. Novák, V. Pokorný, J. Kolorenč, R. Arita, and J. Kuneš, Phys. Rev. B **93**, 035129 (2016).
[24] P. Werner, A. Comanac, L. de' Medici, M. Troyer, and A. J. Millis, Phys. Rev. Lett. **97**, 076405 (2006).
[25] A. Albuquerque, F. Alet, P. Corboz, P. Dayal, A. Feiguin, S. Fuchs, L. Gamper, E. Gull, S. Gürtler, A. Honecker *et al.*, J. Magn. Magn. Mater. **310**, 1187 (2007).
[26] J. E. Gubernatis, M. Jarrell, R. N. Silver, and D. S. Sivia, Phys. Rev. B **44**, 6011 (1991).
[27] See Supplemental Material at http://link.aps.org/supplemental/10.1103/PhysRevLett.116.256403 for explicit calculations.
[28] J. Kuneš, Phys. Rev. B **90**, 235140 (2014).
[29] T. Kaneko and Y. Ohta, Phys. Rev. B **90**, 245144 (2014).
[30] T. Kaneko, B. Zenker, H. Fehske, and Y. Ohta, Phys. Rev. B **92**, 115106 (2015).
[31] S. Hoshino and P. Werner, Phys. Rev. B **93**, 155161 (2016).
[32] The site index was dropped for the sake of simplicity.
[33] Without specifying the orbital shapes we only distinguish the cases with $\mathbf{m}(\mathbf{r}) = 0$ and $\mathbf{m}(\mathbf{r}) \neq 0$.
[34] Assuming the underlying orbitals are real functions.
[35] J. Chaloupka and G. Khaliullin, Phys. Rev. Lett. **116**, 017203 (2016).
[36] C. Zener, Phys. Rev. **82**, 403 (1951).
[37] $|\boldsymbol{\phi}|/s \to 1$ when going from FMEC phase to a ferromagnet formed from purely HS states.